HHS Public Access

Author manuscript

AJR Am J Roentgenol. Author manuscript; available in PMC 2016 August 01.

Published in final edited form as:

AJR Am J Roentgenol. 2015 August ; 205(2): 331–336. doi:10.2214/AJR.14.14221.

Apparent Diffusion Coefficient Values of the Benign Central Zone of the Prostate: Comparison With Low- and High-Grade Prostate Cancer

Rajan T. Gupta[1], **Christopher R. Kauffman**[1], **Kirema Garcia-Reyes**[1], **Mark L. Palmeri**[2], **John F. Madden**[3], **Thomas J. Polascik**[4], and **Andrew B. Rosenkrantz**[5]

[1]Department of Radiology, Duke University Medical Center, DUMC Box 3808, Durham, NC 27710

[2]Department of Biomedical Engineering, Duke University, Durham, NC

[3]Department of Pathology, Duke University Medical School, Durham, NC

[4]Division of Urologic Surgery, Department of Surgery and Duke Prostate Center, Duke University Medical Center, Durham, NC

[5]Department of Radiology, New York University Langone Medical Center, New York, NY

Abstract

Objective—The apparent diffusion Coefficient (ADC) values for benign central zone (CZ) of the prostate were compared with ADC values of benign periphral zone (PZ), benign transition zone (TZ), and prostate cancer, using histopathologic findings from radical prostatectomy as the reference standard.

Materials and Methods—The study included 27 patients with prostate cancer (mean [± SD] age, 60.0 ± 7.6 years) who had 3-T endorectal coil MRI of the prostate performed before undergoing prostatectomy with whole-mount histopathologic assessment. Mean ADC values were recorded from the ROI within the index tumor and within benign CZ, PZ, and TZ, with the use of histopathologic findings as the reference standard. ADC values of the groups were compared using paired *t* tests and ROC curve analysis.

Results—The ADC of benign CZ in the right (1138 ± 123 × 10^{-6} mm^2/s) and left (1166 ± 141 × 10^{-6} mm^2/s) lobes was not significantly different ($p = 0.217$). However, the ADC of benign CZ (1154 ± 129 × 10^{-6} mm^2/s) was significantly lower ($p < 0.001$) than the ADCs of benign PZ (1579 ± 197 × 10^{-6} mm^2/s) and benign TZ (1429 ± 180 × 10^{-6} mm^2/s). Although the ADC of index tumors (1042 ± 134 × 10^{-6} mm^2/s) was significantly lower ($p = 0.002$) than the ADC of benign CZ there was no significant difference ($p = 0.225$) between benign CZ and tumors with a Gleason score of 6 (1119 ± 87 × 10^{-6} mm^2/s). In 22.2% of patients (6/27), including five patients who had tumors with a Gleason score greater than 6, the ADC was lower in benign CZ than in the index tumor. The AUC of ADC for the differentiation of benign CZ from index tumors was 72.4%

Address correspondence to R. T. Gupta (rajan.gupta@duke.edu).

(sensitivity, 70.4%; specificity, 51.9%), and the AUC of ADC for differentiation from tumors with a Gleason score greater than 6 was 76.7% (sensitivity, 75.0%; specificity, 65.0%).

Conclusion—The ADC of benign CZ is lower than the ADC of other zones of the prostate and overlaps with the ADC of prostate cancer tissue, including high-grade tumors. Awareness of this potential diagnostic pitfall is important to avoid misinterpreting the normal CZ as suspicious for tumor.

Keywords

central zone; multiparametric prostate MRI; prostate cancer

The original characterization of the zonal anatomy of the prostate described three distinct zones [1]: the peripheral zone (PZ), the transition zone (TZ), and the central zone (CZ). The PZ and TZ comprise the bulk of the glandular content of the prostate and are the site of the overwhelming majority of prostate cancers [2–4]. Accordingly, these zones have received the greatest degree of attention in prior reports [5]. The CZ, which has received less emphasis, comprises a disk of tissue situated between the PZ and TZ at the posterior base of the prostate below the seminal vesicles, encircling the ejaculatory ducts as they course toward the verumontanum [6]. This histologically distinct zone is a remnant of the wolffian duct [7] and is the site of fewer than 5% of prostate tumors [2, 8]. Partial effacement of the CZ by the TZ, which occurs as the TZ enlarges with aging, can lead to difficulty in differentiating these zones on imaging; because of this difficulty, historically these two zones were often considered a single entity known as the central gland [9, 10].

More recently, improvements in the image quality of prostate MRI and growing clinical interest in precise tumor localization using imaging have led to greater attention being given to the MRI characteristics of the CZ [11]. For instance, one study reported that the CZ can in fact be visualized separately from the TZ in more than 80% of patients [6]. However, distinct visualization of the CZ can, in turn, lead to a diagnostic pitfall, particularly for less-experienced readers. This diagnostic difficulty occurs because the CZ exhibits homogeneous decreased T2 signal and, when visualized separately from the TZ, may be misinterpreted as a lesion suspicious for tumor on T2-weighted images. Avoidance of this pitfall requires awareness of the expected location and morphologic features of the CZ on T2-weighted images, in combination with careful review of the zonal anatomy in the prostate base to appropriately recognize the CZ as a normal structure [6, 11].

Benign CZ prostate tissue has also been described as appearing hypointense on the apparent diffusion Coefficient (ADC) map derived from DWI [6, 12]. Thus, the CZ may pose a diagnostic challenge not just on T2-weighted images but also for the ADC map. In fact, this challenge may be more problematic on the ADC map because of the anatomic distortion and warping of DWI related to both the echo-planar imaging acquisition [13] and subsequent decreased anatomic clarity of this sequence. Although visually decreased ADC in the CZ has been described subjectively in previous studies [6, 12], quantitative ADC values of benign CZ tissue have not been previously investigated, to our knowledge. Such information is important if quantitative ADC measurements and ADC thresholds are applied during clinical assessment of the prostate by MRI, to help avoid misinterpretation of the CZ as a

possible tumor given its decreased ADC. Therefore, the purpose of this study is to compare the ADC values of benign CZ tissue with the ADC values of prostate cancer and of benign tissue in the PZ and TZ, with use of histopathologic findings from whole-mount radical prostatectomy assessment as the reference standard.

Materials and Methods

Patients

In this HIPAA-compliant study, patients with biopsy-proven prostate cancer who were considered candidates for radical prostatectomy provided signed informed consent to be included in an institutional review board–approved prospective database before undergoing 3-T MRI of the prostate performed using an endorectal coil. Additional institutional review board approval was subsequently received for retrospective database query and analysis. The database was initially searched for all patients who had undergone radical prostatectomy and MRI of the prostate performed at Duke University Medical Center between January 2011 and June 2012, and 41 patients were identified. Patients were then excluded from the study for the following reasons: marked susceptibility artifact related to hip arthroplasty noted on DWI (n = 1); no index lesion identified on histopathologic assessment of the prostatectomy specimen (n = 4), as described later; and lack of availability of whole-mount histopathologic findings (n = 9). After these exclusions, the final cohort included 27 patients (mean [± SD] age, 60.0 ± 7.6 years; range, 47–71 years). The mean interval between MRI and surgery was 29.0 ± 39.2 days (range, 1–153 days).

Multiparametric MRI Technique

All imaging was performed using a 3-T MRI scanner (Signa HDxt 3.0T, GE Healthcare) with a single-channel endorectal coil (eCoil, Medrad) used in combination with multichannel phased-array body surface coils. Examinations included multiplanar fast spin-echo T2-weighted imaging (TR/TE, 3950/102; FOV, 160 × 160 mm; axial matrix, 448 × 360; coronal matrix, 384 × 230; slice thickness, 3 mm; three averages; parallel imaging factor, 3) and single-shot echo-planar imaging fat-suppressed DWI (TR/TE, 3500/69.5; FOV, 160 × 160 mm; matrix, 80 × 128; slice thickness, 3 mm; six averages; parallel imaging factor, 3; b values, 0 and 800 s/mm^2). The ADC maps were generated by the scanner console using a standard monoexponential fit. Dynamic contrast-enhanced MRI was also performed, but it was not formally assessed as part of this study.

Whole-Mount Histopathologic Assessment

All prostatectomies were performed by a single fellowship-trained urologic surgeon with more than 20 years of experience in urologic oncology surgery. The prostate specimens were weighed, inked using different colors for the left and right sides, fixed in formaldehyde, and placed overnight in a refrigerator at 4°C. After shaving of the apex and bladder neck margin, the remaining prostate tissue was sectioned in 3- to 4-mm cuts made perpendicular to the surface plane of the rectum and used to prepare whole-mount slices for microscopic assessment [14]. Tissue was marked using H and E stain. A fellowship-trained genitourinary pathologist with more than 20 years of experience reviewed the slides and outlined in ink all the tumor foci, also providing for each tumor the Gleason score and

primary zonal location (which was defined as the zone comprising the greatest fraction of the tumor's area). The pathologist also designated the index tumor for each case [15–17]; the index tumor was considered to be the tumor focus with the highest grade or, when multiple tumor foci with the same grade were present, the largest such tumor focus. Patients with only scattered foci of a Gleason 3 + 3 tumor, with all foci having a diameter of up to 3 mm, were designated as having no index tumor.

Quantitative Analysis

A single fellowship-trained radiologist with 3 years of experience in MRI of the prostate reviewed the MR images in conjunction with scanned high-resolution digital representations of the whole-mount histopathologic slides indicating the location of the index tumor for each patient. ROIs were placed on the ADC map within the index tumor as well as within benign CZ, PZ, and TZ for each patient. ROIs within the index tumor and benign prostate tissue were placed according to the whole-mount histopathologic data and using the T2-weighted image for anatomic reference (Fig. 1). Mean ADC values were recorded for each ROI. For each patient, the ROI within the index lesion was placed on a single axial slice on the ADC map, with the slice in which the tumor appeared to be the largest and most conspicuous selected for this purpose. For the zonal ROIs within benign prostate tissue, one ROI was placed in each lobe in an area free of tumor on histopathologic assessment, with the results between the two lobes averaged. The ROI for benign CZ was placed just below the insertion of the seminal vesicles at the prostatic base, at the location where the CZ has the greatest cross-sectional diameter on axial images and generally is most conspicuous. For three patients in whom tumor was present within or in close proximity to the CZ on a given side, only the contralateral benign CZ was measured. Mean ROI sizes were as follows: for index tumors, 79.5 ± 54.3 mm^2 (range, 27–234 mm^2); for benign CZ, 99.0 ± 54.9 mm2 (range, 33–248 mm^2); for benign PZ, 48.6 ± 26.1 mm^2 (range, 13–103 mm^2); and for benign TZ, 45.5 ± 45.7 m m ^{2} (range, 10– 218 mm^2).

Statistics

For patients for whom ADC values for benign CZ in both the right and left lobes were measured, these two values were compared using paired *t* tests, and the mean absolute difference and relative difference (defined as the absolute difference divided by the average) in the ADC values of for benign CZ between the two lobes was computed. The mean ADC value of the benign CZ was compared with the mean ADC values of the index tumors and both benign PZ and TZ, by use of paired *t* tests. Additional comparisons between the ADC values of normal CZ and index tumors with a Gleason score of 6 and those with a Gleason score greater than 6 were performed using paired *t* tests. Overlap between the ADC values of normal CZ and the index tumor was assessed on a patient-by-patient basis. Finally, ROC curve analysis was performed to assess differentiation of benign CZ and index tumors using ADC values. The *p* values were two sided and considered statistically significant at $p < 0.05$. Statistical assessment was performed with software (MedCalc version 12.7 for Windows, MedCalc Software).

Results

The Gleason scores of the index tumors were as follows: 3 + 3 for 22.2% of patients (6/27), 3 + 4 for 48.1% of patients (13/27), 4 + 3 for 22.2% of patients (6/27), and 4 + 4 for 3.7% of patients (1/27). The zonal locations were as follows: PZ in 81.4% of patients (22/27), TZ in 11.1% of patients (3/27), both PZ and TZ in 3.7% of patients (1/27), and both PZ and CZ in 3.7% of patients (1/27).

Figure 2 summarizes the results of the ROI assessments of the ADC maps, and Figure 3 shows a representative case. The mean ADC for benign CZ was not significantly different between the two lobes ($1138 \pm 123 \times 10^{-6}$ mm^2/s for the right lobe vs $1166 \pm 141 \times 10^{-6}$ mm^2/s for the left lobe; $p = 0.217$). The mean difference in ADC values for benign CZ in the right and left lobes was $85 \pm 74 \times 10^{-6}$ mm^2/s (relative difference, 7.4% ± 6.5%). However, the mean ADC value of benign CZ ($1154 \pm 129 \times 10^{-6}$ mm^2/s) was significantly lower than that of benign tissue in both the PZ ($1579 \pm 197 \times 10^{-6}$ mm^2/s; $p < 0.001$) and the TZ ($1429 \pm 180 \times 10^{-6}$ mm^2/s; $p < 0.001$).

The mean ADC value of the index tumors ($1042 \pm 134 \times 10^{-6}$ mm^2/s) was significantly lower than that of benign CZ ($p = 0.002$). After stratification by tumor grade, although the ADC value of index tumors with a Gleason score greater than 6 ($1014 \pm 139 \times 10^{-6}$ mm^2/s) was significantly lower than the ADC value of benign CZ ($p = 0.004$), there was no significant difference ($p = 0.225$) between the ADC values of tumors with a Gleason score of 6 ($1120 \pm 87 \times 10^{-6}$ mm^2/s) and benign CZ.

Substantial overlap existed between the ADC value of benign CZ and the ADC value of index tumors, including tumors with a Gleason score greater than 6. In 22.2% of patients (6/27), the ADC of benign CZ was lower than that of index tumors; these tumors exhibited Gleason scores as follows: 3 + 3 ($n = 1$), 3 + 4 ($n = 3$), and 4 + 3 ($n = 2$) (Fig. 4). In an additional 37.0% of patients (10/27), the ADC of benign CZ was less than 10% higher than the ADC of the index tumors; these tumors exhibited Gleason scores were as follows: 3 + 3 ($n = 4$), 3 + 4 ($n = 3$), and 4 + 3 ($n = 3$). Furthermore, the AUC for differentiating benign CZ and index tumors was 72.4%, with a threshold value of 1126×10^{-6} mm^2/s providing a sensitivity of 70.4% (19/27) and specificity of 51.9% (14/27). If only index tumors with a Gleason score greater than 6 are considered, then the AUC was 76.7%, with a threshold value of 1123×10^{-6} mm^2/s providing a sensitivity of 75.0% (15/20) and a specificity of 65.0% (13/20).

Discussion

Previous authors have described a potential challenge in interpretation of prostate MRI resulting from the benign CZ given its decreased T2 signal that potentially mimics tumor [6, 11]. In this article, we also describe significantly lower ADC values in the CZ than in both the PZ and TZ. These decreased ADC values were comparable with those of tumors with a Gleason score of 6. Although tumors with a Gleason score greater than 6 had lower ADC values on average than did benign CZ tissue, substantial overlap existed with this group as

well. The presence of decreased ADC in benign CZ has been attributed to its relatively compact stroma and decreased luminal fluid content [12].

Although past studies describe a lower ADC in the CZ during subjective visual assessment, this study is, to our knowledge, the first to quantify such ADC values and perform separate comparisons with histologically proven low- and high-grade tumors. Such quantitative comparisons are important given increasing interest in clinical application of specific ADC thresholds to guide interpretation of prostate MRI [18]. To apply a particular threshold, ROIs must be placed to measure the ADC within suspicious regions, with the obtained values affecting the level of suspicion that is ultimately raised for tumor. This approach will generate false-positive interpretations for tumor if the CZ is not recognized as a normal anatomic structure and its ADC value is evaluated in such a fashion.

To address this challenge, the interpreting radiologist may assess for a symmetric reduction of ADC at the posterior base of the prostate to support benign CZ tissue as the explanation of the imaging finding, as is borne out by the similar mean values between the two CZ lobes in our study. Nonetheless, enlargement of the TZ at the base of the prostate as a result of benign prostatic hyperplasia may result in displacement of one of the lobes of the CZ, leading to asymmetry [19]. An additional consideration is that benign CZ typically exhibits a type 1 or type 2 kinetic curve using dynamic contrast-enhanced MRI, such that the presence of a type 3 curve may be used to more reliably suggest the presence of tumor [12]. Ultimately, findings in this region of the prostate on the ADC map and dynamic contrast-enhanced MRI must be carefully evaluated in combination with anatomic details apparent on T2-weighted images to mitigate the likelihood of a misinterpretation. We acknowledge that, in a fraction of examinations, it may remain difficult to reliably differentiate asymmetry of benign CZ from tumor by imaging and that targeted biopsy of the area may be needed to establish the diagnosis.

Our study has limitations. First, this was a retrospective study with a relatively small sample size. However, we applied stringent inclusion criteria that required all patients' prostatectomy specimens to undergo whole-mount histopathologic assessment with identification of an index lesion to improve the reliability of the radiologicpathologic correlations. In addition, we were not able to compare ADC values between benign tissue and tumors in the CZ given the lack of tumors located primarily in the CZ in our cohort. Nonetheless, this is an important avenue for future research. Also, observations were performed by a single radiologist who was experienced in prostate MRI. However, the observations were quantitative in nature and were directly guided by knowledge of the histopathologic findings, thereby reducing the subjectivity of the measurements. In addition, only mean ADC values were evaluated, consistent with our intent to reveal an important diagnostic pitfall when using a standard clinical interpretation scheme. Although not widely used in clinical practice, histogram-based whole-lesion ADC metrics have shown added value in comparison with the mean ADC in some investigations [20–22], and these metrics warrant attention for evaluation of benign and malignant CZ as well. Finally, DWI was performed using a maximal b value of 800 s/mm^2, whereas recent literature supports the use of greater b values [23, 24]. The b value used in our study reflects the protocol in use at Duke University at the time that the patients who were included in the study underwent

imaging. Future studies could assess for potential improved differentiation of benign CZ from that of prostate cancer when using larger b values.

In conclusion, the benign CZ of the prostate exhibits significantly lower ADC values than does both benign PZ and TZ and substantially overlaps with ADC values of prostate cancer. Although high-grade tumors tended to exhibit lower ADC values than benign CZ, overlap between benign CZ and tumor existed as well. Such overlap can contribute to a false-positive interpretation for tumor at the prostate base. ADC values in the CZ were similar between the two lobes in a given patient, which may be useful in correctly identifying this structure. Ultimately, thorough familiarity with the normal anatomy of the prostate and with the characteristic appearance of the CZ on multiparametric MRI is required to recognize this pitfall and avoid a misinterpretation.

Acknowledgments

We thank Andrew Buck, Evan Kulbacki, and Kathryn R. Nightingale for their contributions to this work.

Part of this work was funded through grant support from the Wallace H. Coulter Foundation via the Duke-Coulter Translational Partnership Grant Program and also through the National Institutes of Health (grant R01CA142824).

References

1. McNeal JE. The zonal anatomy of the prostate. Prostate. 1981; 2:35–49. [PubMed: 7279811]
2. McNeal JE, Redwine EA, Freiha FS, Stamey TA. Zonal distribution of prostatic adenocarcinoma: correlation with histologic pattern and direction of spread. Am J Surg Pathol. 1988; 12:897–906. [PubMed: 3202246]
3. Noguchi M, Stamey TA, McNeal JE, Yemoto CE. An analysis of 148 consecutive transition zone cancers: clinical and histological characteristics. J Urol. 2000; 163:1751–1755. [PubMed: 10799175]
4. Stamey TA, Donaldson AN, Yemoto CE, McNeal JE, Sözen S, Gill H. Histological and clinical fndings in 896 consecutive prostates treated only with radical retropubic prostatectomy: epidemiologic significance of annual changes. J Urol. 1998; 160:2412–2417. [PubMed: 9817394]
5. Barentsz JO, Richenberg J, Clements R, et al. ESUR prostate MR guidelines 2012. Eur Radiol. 2012; 22:746–757. [PubMed: 22322308]
6. Vargas HA, Akin O, Franiel T, et al. Normal central zone of the prostate and central zone involvement by prostate cancer: clinical and MR imaging implications. Radiology. 2012; 262:894–902. [PubMed: 22357889]
7. Quick CM, Gokden N, Sangoi AR, Brooks JD, McKenney JK. The distribution of PAX-2 immunoreactivity in the prostate gland, seminal vesicle, and ejaculatory duct: comparison with prostatic adenocarcinoma and discussion of prostatic zonal embryogenesis. Hum Pathol. 2010; 41:1145–1149. [PubMed: 20413145]
8. Cheng L, Jones TD, Pan CX, Barbarin A, Eble JN, Koch MO. Anatomic distribution and pathologic characterization of small-volume prostate cancer (<0.5 ml) in whole-mount prostatectomy specimens. Mod Pathol. 2005; 18:1022–1026. [PubMed: 15861213]
9. Zechmann CM, Simpfendorfer T, Giesel FL, et al. Comparison of peripheral zone and central gland volume in patients undergoing intensity-modulated radiotherapy. J Comput Assist Tomogr. 2010; 34:739–745. [PubMed: 20861778]
10. Oto A, Kayhan A, Jiang Y, et al. Prostate cancer: differentiation of central gland cancer from benign prostatic hyperplasia by using diffusion-weighted and dynamic contrast-enhanced MR imaging. Radiology. 2010; 257:715–723. [PubMed: 20843992]
11. Rosenkrantz AB, Taneja SS. Radiologist, be aware: ten pitfalls that confound the interpretation of multiparametric prostate MRI. AJR. 2014; 202:109–120. [PubMed: 24370135]

12. Hansford BG, Karademir I, Peng Y, et al. Dynamic contrast-enhanced MR imaging features of the normal central zone of the prostate. Acad Radiol. 2014; 21:569–577. [PubMed: 24703469]
13. Alexander AL, Tsuruda JS, Parker DL. Elimination of eddy current artifacts in diffusion-weighted echo-planar images: the use of bipolar gradients. Magn Reson Med. 1997; 38:1016–1021. [PubMed: 9402204]
14. Fitzsimons NJ, Sun LL, Dahm P, et al. A single-institution comparison between radical perineal and radical retropubic prostatectomy on perioperative and pathological outcomes for obese men: an analysis of the Duke Prostate Center database. Urology. 2007; 70(114):6–1151.
15. Ahmed HU. The index lesion and the origin of prostate cancer. N Engl J Med. 2009; 361:1704–1706. [PubMed: 19846858]
16. Bott SR, Ahmed HU, Hindley RG, Abdul-Rahman A, Freeman A, Emberton M. The index lesion and focal therapy: an analysis of the pathological characteristics of prostate cancer. BJU Int. 2010; 106:1607–1611. [PubMed: 20553262]
17. Gupta RT, Kauffman CR, Polascik TJ, Taneja SS, Rosenkrantz AB. The state of prostate MRI in 2013. Oncology (Williston Park). 2013; 27:262–270. [PubMed: 23781689]
18. Chamie K, Sonn GA, Finley DS, et al. The role of magnetic resonance imaging in delineating clinically significant prostate cancer. Urology. 2014; 83:369–375. [PubMed: 24468511]
19. Yu J, Fulcher AS, Turner MA, Cockrell CH, Cote EP, Wallace TJ. Prostate cancer and its mimics at multiparametric prostate MRI. Br J Radiol. 2014; 87:20130659. [PubMed: 24646125]
20. Donati OF, Mazaheri Y, Afaq A, et al. Prostate cancer aggressiveness: assessment with whole-lesion histogram analysis of the apparent diffusion Coefficient. Radiology. 2014; 271:143–152. [PubMed: 24475824]
21. Peng Y, Jiang Y, Antic T, Giger ML, Eggener SE, Oto A. Validation of quantitative analysis of multiparametric prostate MR images for prostate cancer detection and aggressiveness assessment: a cross-imager study. Radiology. 2014; 271:461–471. [PubMed: 24533870]
22. Rosenkrantz AB, Triolo MJ, Melamed J, Rusinek H, Taneja SS, Deng FM. Whole-lesion apparent diffusion Coefficient metrics as a marker of percentage Gleason 4 component within Gleason 7 prostate cancer at radical prostatectomy. J Magn Reson Imaging. 2014; 41:708–714. [PubMed: 24616064]
23. Metens T, Miranda D, Absil J, Matos C. What is the optimal b value in diffusion-weighted MR imaging to depict prostate cancer at 3T? Eur Radiol. 2012; 22:703–709. [PubMed: 21971824]
24. Katahira K, Takahara T, Kwee TC, et al. Ultra-high-b-value diffusion-weighted MR imaging for the detection of prostate cancer: evaluation in 201 cases with histopathological correlation. Eur Radiol. 2011; 21:188–196. [PubMed: 20640899]

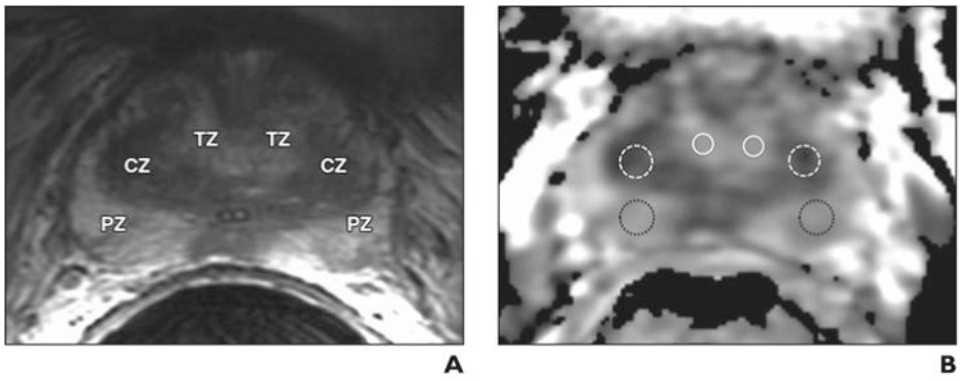

Fig. 1.

Depiction of ROI placement for calculation of mean apparent diffusion Coefficient (ADC) value.

A, Axial T2-weighted image used for anatomic delineation of histologically confirmed benign transition zone (TZ), central zone (CZ), and peripheral zone (PZ).

B, Corresponding axial ADC map with representative ROI placements in each of these zones used for calculation of mean ADC value for benign in TZ (*solid white circles*), CZ (*dashed white circles*), and PZ (*dotted black circles*).

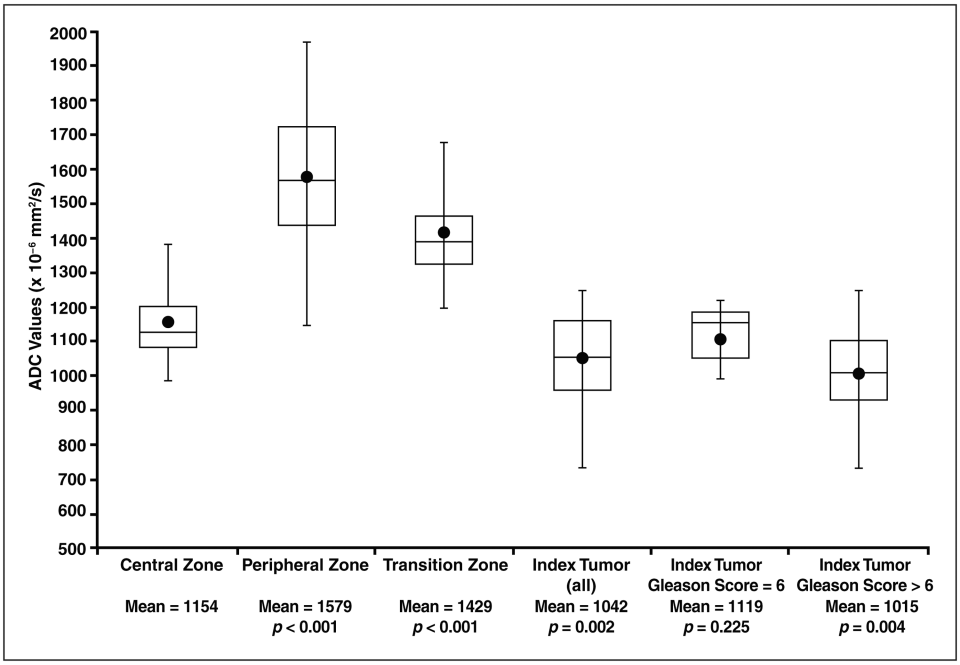

Fig. 2.

Box plots of apparent diffusion Coefficient (ADC) values. Statistically significant differences between ADC values of peripheral zone, transition zone, and index tumor categories versus ADC value of benign central zone (CZ) are shown, with $p < 0.05$ denoting statistical significance. Mean (*circles*), median (*line in box*), second and third quartiles (*top and bottom of boxes*), and maximum values (*whiskers outside of boxes*) are shown.

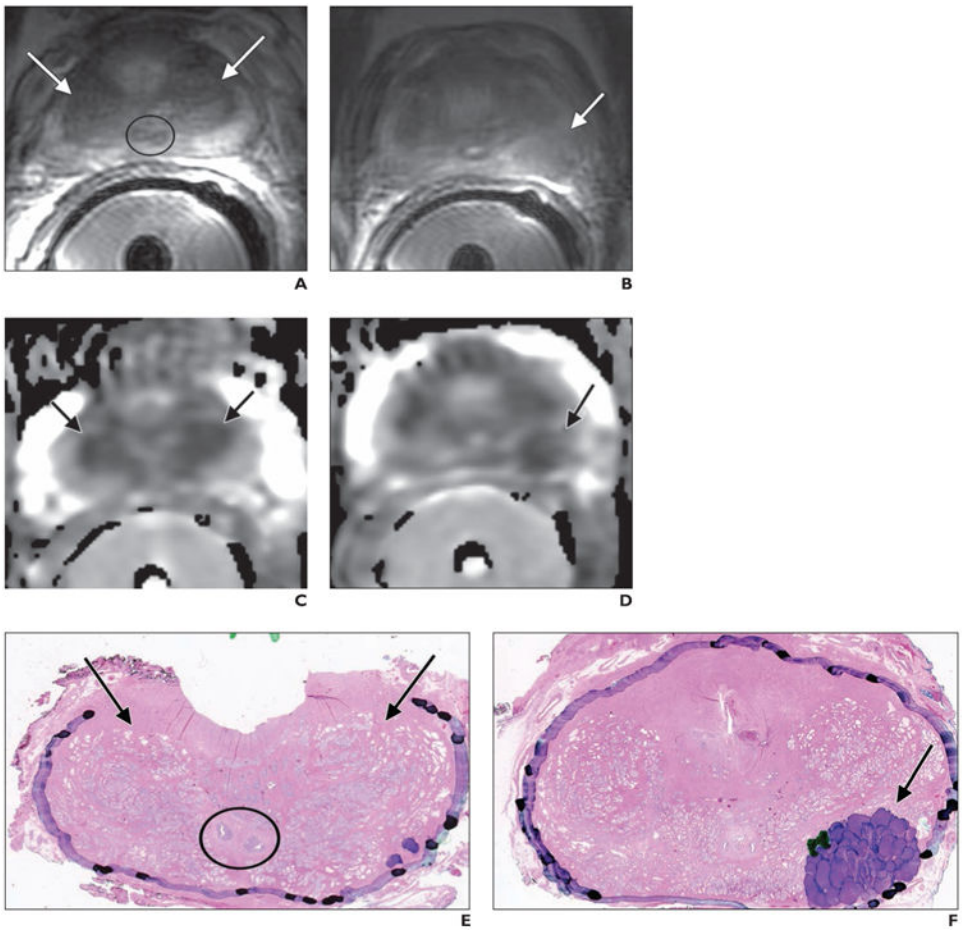

Fig. 3.

52-year-old man with prostate cancer and Gleason score of 4 + 3 at radical prostatectomy.

A, A xial T 2-weighted image shows normal appearance of the central zone (CZ) (*arrows*) at prostate base, situated between peripheral and transition zones and encircling ejaculatory ducts (*circle*).

B, Axial T2-weighted image shows histologically confirmed index tumor (*arrow*) located at left posterior prostate midgland.

C and **D**, Axial apparent diffusion Coefficient (ADC) maps show visually similar extent of decreased ADC (*arrows*) in both CZ (**C**) and index tumor (**D**). Measured ADC values were minimally lower in benign CZ (1036×10^{-6} mm^2/s) than in index tumor (1072×10^{-6} mm^2/s).

E and **F**, Whole-mount histopathologic slides (H and E stain, ×1.05) show benign CZ at base of prostate (*arrows*, E) and index tumor in left posterior midgland (*arrow*, **F**). Ejaculatory ducts (*circle*, **E**) are shown. Purple markings (**F**) denote that majority of tumor has components of Gleason pattern 4, with minority of components of Gleason pattern 3 denoted by dark green markings.

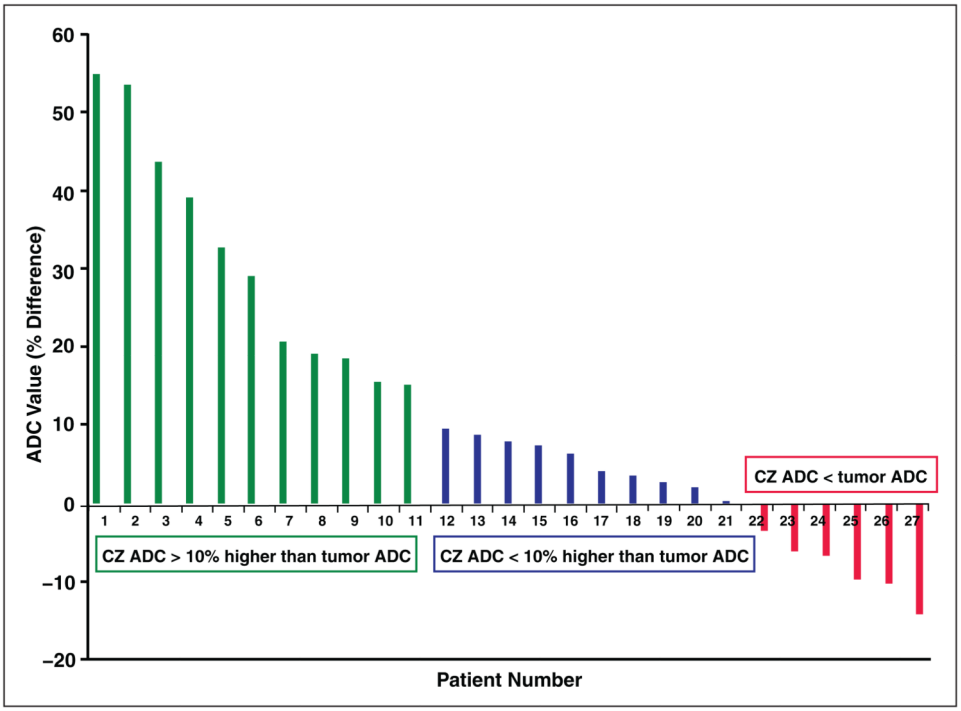

Fig. 4.

Graph of difference in apparent diffusion Coefficient (ADC) values between benign central zone (CZ) and index tumors in 27 patients. For patients 1–11, CZ ADC is > 10% higher than tumor ADC, for patients 12–21, CZ ADC is < 10% higher than tumor ADC; and for patients 22–27, CZ ADC is less than tumor ADC.